

Electro-reduction of CO₂ to HCOOH and CH₃OH over Pd-polyaniline Catalyst in Acidic Solution: A Study of Pd Size Effect

Weiran Zheng^[a], Ho Wing Man^[a], Lin Ye^{*[b]}, Shik Chi Edman Tsang^{*[a,b]}

Abstract: By controlling reaction temperature and feeding rate of reducing agent, it is shown that Pd nanoparticles with different sizes can be synthesized from reduction of their precursor on polyaniline (PANI) as solid carrier. Using UV-Vis spectroscopy, ¹H-NMR, and ATR-IR as characterization tools, electronic and catalytic interactions between Pd NPs and PANI can be clearly identified. It is shown that for the first time that the unique redox properties of Pd/PANI display a high over-potential for hydrogen evolution, suppressing this competitive reaction from electro-reduction of CO₂ in acidic solution. As a result, two main liquid products (HCOOH and CH₃OH) can be selectively produced with only trace amount of CO in gas phase. The current efficiencies for HCOOH and CH₃OH are found to increase with decreasing Pd NPs sizes within the potential range of -0.5 to -0.9 V. The highest current efficiency for HCOOH (22.8 %) and for CH₃OH (5.4%) are thus obtained over Pd(1.31 nm)/PANI at -0.9 V.

Introduction

Conversion of carbon dioxide (CO₂) to small organic molecules has attracted tremendous interests from chemists for decades. Some products, like formic acid (HCOOH) and methanol (CH₃OH) are of particular interests due to their positions as potential fuels for fuel cell related applications.^[1] Among all the conversion methods, electrocatalytic reduction is one of the most promising methods due to the mild conditions and sustainable energy resources that can be used. The recent dwindling cost of grids from renewable energies such as solar, hydropower and biomass makes the process even more appealing. Many materials were extensively explored in order to identify a suitable electrocatalyst for CO₂ reduction to useful products, including organic molecules, ionic liquids, metal complexes, metal salts, and perhaps the most studied material: metal nanoparticles (NPs).^[2-4] Early studies showed that Ag, Pb, Zn, Pd, and Cu metals as electrodes can produce mainly carbon monoxide, CH₃OH and HCOOH with trace amounts of methane (CH₄), ethylene (C₂H₄) and higher hydrocarbons from CO₂ electro-reduction in aqueous solution.^[5,6] Although the reaction mechanism for the electro-reduction on metal surface has been discussed in some recent works,^[7,8] it still remains obscure how the morphology of metal NPs would affect the CO₂ reaction with reference to activity and selectivity, making the rational design of a selected electro-catalyst for this reaction even harder.

The difficulties of using metal NPs for CO₂ electro-reduction reaction lie in their high over-potential and poor selectivity to useful products. Pd is one of the few metals, which shows relatively lower potential with higher product selectivity over a wide range metal NPs studied. The common products by using Pd based electro-catalysts are HCOOH, CO and H₂.^[9,10] The proportion of these products formed largely depends on the reaction conditions (electrolyte type, pH et al) and the morphology of Pd NPs used. Notably, most of the CO₂ reductions were performed in basic (HCO₃⁻) solution in the literature, although in few cases, acidic conditions were reported. Koper et al. demonstrated that HCOOH can be produced in high current density from acidic solution (pH = 2) pre-saturated with CO₂, although they also showed that CO poisoning is taken place during the reaction.^[10] Bao and his co-workers reported the study of pH effect on CO₂ reduction over Pd nanoparticles (NPs). They could suppress the CO formation but were unable to reduce the hydrogen evolution.^[11] Thus, it would be ideal to use acidic conditions provided that the competitive hydrogen evolution reaction can be suppressed.

The size effect of metal NPs is one of the recent hottest topics in catalysis and electrocatalysis because of the dramatic electronic and surface changes associated with particular sizes of NPs.^[12] Although such effect was widely studied in electrochemical reactions^[13], few works have been performed on the CO₂ electro-reduction. Bao et al. were amongst the first research groups to report on a size-dependent activity/ selectivity in the electrocatalytic reduction of CO₂ using Pd NPs. They found that smaller NPs gave higher CO current efficiency in 0.1 M KHCO₃ solution.^[14] As far as we are aware, there is no report in open literature on the size effect study of Pd NPs in acidic condition, presumably due to massive hydrogen production overriding other products formation from the severe hydrogen evolution reaction (HER) in acidic solution.

In order to stabilize Pd NPs and decrease the HER reaction, support with controlled electronic and proton conductivity may be introduced. From this respect, an interesting conductive polymer, polyaniline (PANI) has attracted our attention. The redox properties between its semi-conductive and conductive states may fulfil the needs as the support for Pd NPs in acid solution^[15]. The basic nitrogen containing moieties may also bind CO₂ by Lewis acid-base interaction in the PANI backbone^[16]. This enables the PANI based catalysts to capture CO₂ favourably in the electrochemical environment^[17]. Pd NPs supported on PANI has initially been reported as an efficient CO₂ electro-reduction catalyst. Wang et al. reported that a Pd-polyaniline/CNT nanohybrids in KHCO₃ solution can give high current efficiency for COOH⁻ with a small amount of CO produced.^[18] It would be therefore interesting to study the Pd/PANI based catalysts with different Pd sizes under acidic conditions.

[a] W. Zheng, H.W. Man, S.C.E. Tsang*
Department of Applied Biology and Chemical Technology, Hong Kong Polytechnic University, Hong Kong, China
E-mail: edman.tsang@chem.ox.ac.uk

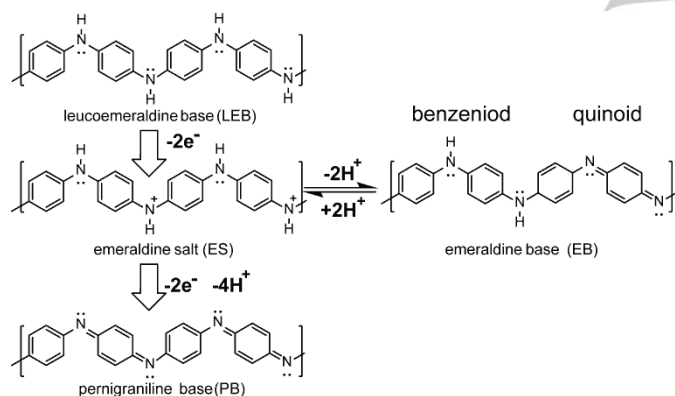
[b] L. Ye* and S.C.E. Tsang
Department of Chemistry, University of Oxford, UK. OX1 3QR.
E-mail: lin.ye@chem.ox.ac.uk

Here, in this paper, we have investigated the effect of Pd particle size by preparing differently sized Pd NPs in PANI for the CO₂ electro-reduction in acidic solution. The unique nanofiber structure with surface doped with Pd NPs of variable sizes has been achieved. UV-Vis spectroscopy, ¹H-NMR and ATR-IR techniques have been employed to probe the interaction(s) between Pd NPs and PANI. The over-potentials of HER in acidic media have also been particularly evaluated for PANI and Pd/PANI. The performances in CO₂ electro-reduction of PANI using differently sized Pd NPs have been compared, which shows a good correlation of activity-structure relationship for the Pd/PANI materials.

Results and Discussion

Morphology and structure of PANI and Pd/PANI

PANI is a widely studied conductive polymer with many interesting properties which include facilitated multi-step redox modes, as shown in Scheme 1.^[19] PANI can go through two stages of redox reactions from totally reduced form (leucoemeraldine base, LEB) to half oxidized form (emeraldine base, EB), then to fully oxidized form (pernigraniline base, PB). The degree of oxidation can be indicated by the ratio between benzenoid and quinoid structures. In acidic condition, EB can take up two protons to yield a conjugate form, emeraldine salt.^[15]



Scheme 1. Redox modes of polyaniline.

In our study, PANI was prepared using a rapidly mixing method in HCl aqueous solution according to Huang and colleagues.^[20] After de-doping process by washing the as-synthesized, green PANI with NH₃·H₂O, the blue powder of PANI (EB form) was obtained. To simplify the definition of variable states, PANI after this treatment is predominantly in the EB form. PANI powder (2 mmol of repeating unit, EB form) was dispersed in 25 mL DMF and sonicated for 30 min. Then, (NH₄)₂PdCl₄ (0.4 mmol) was added to the suspension to prepare metal/PANI (molar ratio of metal/N = 1:5), followed by adding sodium borohydride, NaBH₄ in DMF solution as reducing agent. The rate of adding reducing agent and reaction temperature were controlled to produce Pd NPs with different sizes, the synthesis temperature, and NaBH₄ adding rate parameters are summarized in Table 1.

Table 1. Details of Pd/PANI samples.

Sample name	Reduction temperature	NaBH ₄ adding rate (1 mg mL ⁻¹ in DMF)	Mean diameter
Pd-1/PANI	80 °C	1.0 mL min ⁻¹	1.31 nm
Pd-2/PANI	25 °C	1.0 mL min ⁻¹	2.44 nm
Pd-3/PANI	10 °C	0.1 mL min ⁻¹	9.73 nm

Figure 1a shows the scanning electron microscope (SEM) images of as-prepared PANI and Pd/PANI materials. Figure 1a-i suggests that PANI has nanofiber-like morphology with a diameter of 150 nm to 300 nm, the appearance of which matches with corresponding reports in literature.^[20] After reduction of the Pd precursor, it seems that Pd NPs are doped on the surface of these PANI nanofibers, as shown in Figure 1a-ii. An illustration of Pd/PANI is shown in Figure 1b to demonstrate such morphology. Figure 2 shows the transmission electron microscopy (TEM) images, which reveal the morphological and structural details of the supported Pd nanoparticles by this technique. Figure 2a-i confirms the parent nanofiber-like structure of PANI and Figures 2a-ii, iii and iv show the close-up morphologies of Pd NPs with different mean diameters (D) ranging from 1.31 nm to 2.44 nm and 9.73 nm, respectively. The Pd/PANI samples are christened as Pd-1/PANI (D = 1.31 nm), Pd-2/PANI (D = 2.44 nm) and Pd-3/PANI (D = 9.73 nm) in Table 1. Pd NPs in Pd-2/PANI are not in ideal spherical shape but with worm-like morphology of a mean length of 6.21 nm.

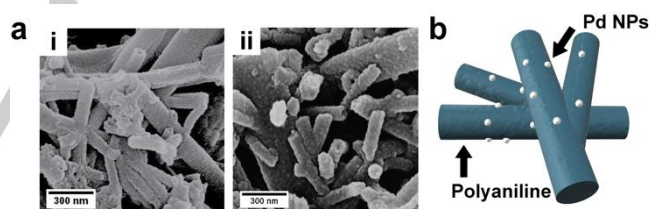


Figure 1. (a) SEM images of i: PANI and ii: Pd-2/PANI. (b) An illustration of Pd/PANI.

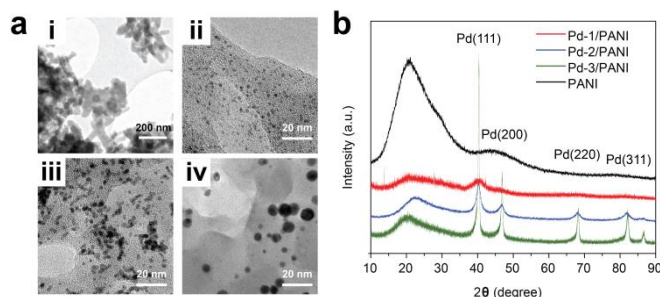


Figure 2. (a) TEM images of i: PANI, ii: Pd-1/PANI, iii: Pd-2/PANI and iv: Pd-3/PANI. (b) XRD patterns of Pd/PANI and PANI.

X-ray powder diffraction (XRD) patterns of PANI and Pd/PANI are also shown in Figure 2b. The characteristic peaks of *fcc* Pd structure can be clearly observable in all Pd/PANI samples. With increasing particle sizes, the corresponding peaks of Pd become sharper. The calculated particle sizes based on Pd(111) peak from Scherrer equation agree well with the values derived from TEM images. PANI is known to possess repeatable chemical backbones of its conjugated benzenoid and quinoid moieties with H-bonding linkage.^[21] The broad peak located at 20.5° ($d = 0.46$ nm) can be assigned to the crystalline structure with the intermolecular H-bonding stacking. As seen from the figure, after Pd precursor is introduced and reduced, this peak shifts from 20.5° to 22.6° in Pd-2/PANI. The increase in 2θ value suggests a decrease in the corresponding d -spacing, hence a higher degree of H-bonding interaction. Pd-1 appears to generate a slightly closer packing of PANI compared to Pd-2 due to more extensive H-bonding introduced by smaller Pd particle size. However, when the size of Pd NPs reaches 9.73 nm as in Pd-3/PANI, the peak position does not seem to shift. In order to further correlate the degree of intermolecular H-bonding packings of PANI units (higher degree with lower quinoid/benzenoid ratio) with the reduction of Pd NPs from the precursor, Raman spectroscopy was also used. It is known that a Raman peak around at 1160 cm^{-1} assigned to vibration of quinoid (oxidized form with lesser intermolecular H bonding) to a peak at 1219 cm^{-1} assigned to vibration of benzenoid (reduced form with higher H bonding) as the peak ratio can be used to assess the redox state of the PANI.^[21] After the Pd-2 metal NPs incorporation, a significant decrease in the Raman peak ratio from 2.88 to 2.67 was indeed recorded (Raman peaks, not shown).

Pd-PANI electronic interactions

The interactions between Pd NPs and PANI were also studied using a number of characterization methods, which included Ultraviolet–visible (UV-Vis) spectroscopy, proton nuclear magnetic resonance ($^1\text{H-NMR}$) and attenuated total reflection infrared spectroscopy (ATR-IR), etc. The results are summarized below:

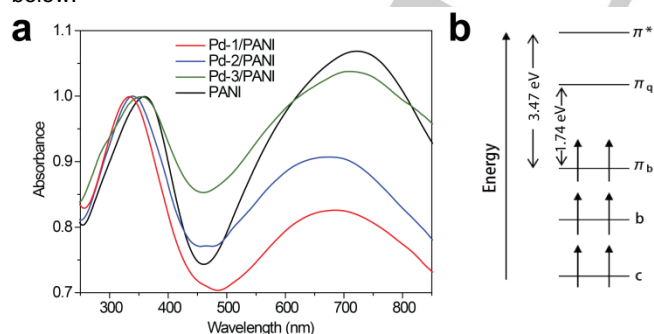


Figure 3. (a) UV-Vis spectra of PANI and Pd/PANI. (b) Schematic energy level diagram of PANI.

Figure 3 shows the UV-vis spectra of PANI and Pd/PANI. In the typical testing, DMF solution was used to disperse PANI and Pd/PANI: the concentration of PANI for all samples was set at

0.05 mg PANI/mL. Figure 3 shows the PANI with two peaks at 357 nm (3.47 eV) and 712 nm (1.74 eV). According to the energy level diagram of PANI, these two peaks can be assigned to electronic excitations.^[22] The peak at 357 nm, is attributed to $\pi_b\text{-}\pi^*$ excitation and the peak at 712 nm is attributed to $\pi_b\text{-}\pi_q$ excitation of their conjugated systems. In the case of Pd/PANI, according to the figure, both peaks shift to a lower wavelength, suggesting higher energies are required for the electronic excitations in both $\pi_b\text{-}\pi^*$ and $\pi_b\text{-}\pi_q$. Such effect can be caused by the decrease in π_b energy level. It is thus reasonable to assume that Pd NPs have an electronic interaction with PANI, donating electrons to PANI's HOMO, lowering the energy level of π_b . Comparing Pd-1/PANI, Pd-2/PANI, and Pd-3/PANI, it is interesting to find that the first peak positions are 331 nm (3.74 eV), 344 nm (3.60 eV) and 352 nm (3.52 eV), respectively. The corresponding energy shifts caused by Pd-1, Pd-2, and Pd-3 to PANI are 0.27 eV, 0.13 eV, and 0.05 eV, suggesting that Pd NPs with smaller size have a stronger electronic effect on π_b energy level. Apart from the peak shift, it is noted that the peak intensity assigned to $\pi_b\text{-}\pi_q$ excitation also decreases with decreasing particle size, while that allocated to $\pi_b\text{-}\pi^*$ remains the same. MacDiarmid et al. showed that the relative peak intensity could be used to estimate the oxidation state of polyaniline, and the decreasing intensity at ~ 700 nm is related to the decreasing quinoid percentage (more reduced PANI).^[23] Thus, our observed changes in Figure 3a clearly reflect that the decreasing proportion of quinoid in the polymer backbone when different sizes of Pd NPs are introduced: Pd NPs with smaller size donate more electrons to PANI, making it more reduced.

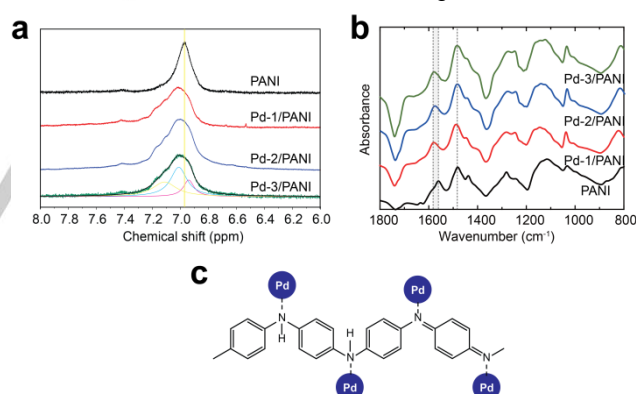


Figure 4. (a) $^1\text{H-NMR}$ spectra of PANI and Pd/PANI in DMSO-d_6 . (b) ATR-IR spectra of PANI and Pd/PANI. (c) Suggested Pd/PANI interaction structure.

Further evidence of the electronic interaction(s) between Pd NPs and PANI is also shown in Figure 4. $^1\text{H-NMR}$ method was used to gauge the change in population of H atoms in -NH- group (7.0–7.2 ppm) of PANI during the formation of Pd NPs. PANI and Pd/PANI were first dispersed in dimethyl sulfoxide- d_6 (DMSO-d_6) with a concentration of 1 mg PANI/mL. The results are shown in Figure 4a. PANI gives a single hump at 6.96 ppm, assigned to the population of N-H protons. After the *in situ* formation of Pd NPs, the peak becomes broader. By peak fitting (an example is shown for Pd-3/PANI spectrum), it is clear that new peaks are arisen with higher chemical shift values, overlapping with the original N-H population of the PANI. These

new peaks suggest an increase in the population and chemical shift values of N-H due to the Pd...N interaction. However, there is only a marginal change in the $^1\text{H-NMR}$ spectra with different Pd NPs sizes. ATR-IR was also used to evaluate the interactions of PANI caused by Pd NPs with different sizes. As shown in Figure 4b, PANI displays two characteristic peaks at 1480 cm^{-1} and 1561 cm^{-1} , respectively. The first peak is assigned to C=C stretching vibrations of benzenoid structure, and the second is assigned to C=N stretching vibration in quinoid structure.^[15] After the *in situ* formation of Pd NPs, the two peaks of PANI retain, indicating that the polymer structure of PANI remains intact during the Pd NPs formation. However, the peak assigned to C=N (quinoid structure) is progressively shifting from 1561 cm^{-1} to $\sim 1576\text{ cm}^{-1}$ according to the material series (PANI, Pd-3, Pd-2, Pd-1) while their C=C peak position virtually remains at the same position (1480 cm^{-1} of PANI, 1484 cm^{-1} of Pd-1/PANI, 1481 cm^{-1} of Pd-2/PANI and 1482 cm^{-1} of Pd-3/PANI). Thus, the above observations indicate that Pd atoms can interact with PANI via nitrogen atoms instead of carbon atoms. A graphical representation of Pd...N interaction in Pd/PANI is summarized in Figure 4c.

Electrochemical properties of PANI and Pd/PANI

The activity of HER was tested over PANI and the series of Pd/PANI materials: their polarization curves and corresponding Tafel plots are shown in Figure 5.

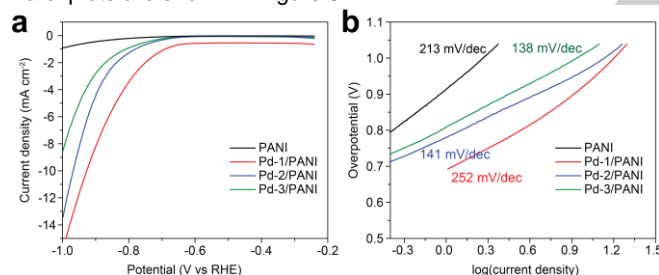


Figure 5. (a) HER polarization curves of PANI and Pd/PANI, the scan rate is 50 mV s^{-1} . (b) The corresponding Tafel plots.

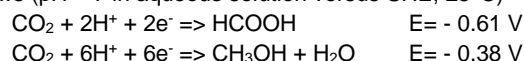
The HER reaction was carried out in $0.5\text{ M H}_2\text{SO}_4$ aqueous solution, and the scan rate was set at 50 mV s^{-1} . The current density was calculated based on the surface area of the glassy carbon electrode. Figure 5a shows that the highest activity of HER is taken place by Pd-1/PANI: PANI doped with Pd NPs with a mean diameter of 1.31 nm . The activity (current density) decreases as particle size increases. For pure PANI, the activity is the lowest. The decreasing activity of Pd/PANI may be explained in two aspects: 1. smaller metal particles give larger electrochemical surface areas to support higher current densities; 2. smaller particles can alter the Fermi level of PANI (π_b , see Figure 3) more strongly, resulting in the higher HER activity. It is well accepted that the HER activity at negative electrode is due to reduction of protons to H atoms on metal surface (i.e. Pd) followed by the recombination of two H atoms to form hydrogen gas: the high conductivity and facilitated metal surface of catalyst will give a good HER activity at lower over-potential. The generally over-potential values of Pd/PANI

materials for the HER are known to be significantly higher than that of Pd/C ($0.15\text{ V} \sim 0.2\text{ V}$).^[25] This is because PANI as a redox support material for Pd NPs is capable of reducing the population of electrons and protons from the Pd metal surface by interacting with the PANI. As a major phase in the electrode, PANI with metallic properties is also active for HER. However, when it will turn from ES to LEB form after extensive reduction, the polymer nanofiber becomes less conductive because of the decreasing conjugated units hence offering extremely high intrinsic over-potential for HER activity (Scheme 1).^[24] Such structural and electronic alterations render the composites interesting to reduce HER activity of Pd NPs in acidic conditions. As shown in Figure 5b, the overall over-potential measured at 1 mA cm^{-2} is 0.67 V for Pd-1/PANI, 0.76 V for Pd-2/PANI, 0.80 V for Pd-3/PANI and 0.91 V for PANI, respectively. It is clear that the lower over-potentials are clearly associated with smaller Pd particle sizes with stronger interactions with the PANI due to their competition for HER. The activity for HER can also be reflected from the slope of Tafel curve: lower Tafel slope indicates higher activity of HER for a given over-potential. Thus, Pd-2/PANI and Pd-3/PANI show substantially higher activity for HER (141 mV/dec and 138 mV/dec , respectively) than PANI (213 mV/dec) for the potential range studied. Although Pd-1/PANI displays as low activity for HER as PANI for a given over-potential within experimental error (252 mV/dec) but its low over-potential (0.67 V) suggests an overwhelming contribution from the electrochemical surface area of this metal-composite due to smallest particle size used.

CO₂ electro-reduction tests

It is noted that HER can be the main competitive reaction in CO₂ electro-reduction, the high overpotential of PANI and Pd/PANI materials would possibly suppress the HER but promote the CO₂ reduction. As a result, the series of Pd/PANI samples with variable Pd NPs sizes were tested for electro-reduction of CO₂.

Catalytic CO₂ electro-reduction has been intensively studied in past few years. The main reported products include CO, CH₄, HCOOH, CH₃OH, higher hydrocarbons, etc. The product selectivity apparently depends critically on nature of catalysts and reaction conditions used. The production to HCOOH and CH₃OH are of particular interests due to their high energy contents as potential fuel products. The reactions are shown as follows (pH = 7 in aqueous solution versus SHE, 25°C)^[26]:



Faradaic efficiency or current efficiency (ϵ) is commonly accepted to gauge the selectivity for CO₂ electro-reduction. The value is the charge fraction used for product generation, and can be calculated based on following equation:

$$\epsilon = z^* n^* F / Q$$

Where: z is the number of electrons used to produce a product, e.g. $z = 2$ for CO₂ reduction to HCOOH. n is the total mole of the product. F is Faraday's constant ($F = 96485\text{ C mol}^{-1}$). Q is the total charge used for the entire electrochemical process.

Firstly, in our experiment, cyclic voltammetry (CV) was used to study the change of current density (total reaction rate) before

and after CO₂ saturation. Rotating disk electrode (RDE) was coated with PANI or Pd/PANI for the electrochemical tests. As shown in Figure 6a, the CV plots of Pd-2/PANI in acidic solution under N₂ and CO₂ conditions are presented. A broad peak is visible at 0 - 0.2 V under the two different gases. This peak is assigned to the first reduction peak of PANI (EB to LEB).^[27] Comparing to the N₂ curve, the value of current density decreases at negative potentials after the solution is saturated with CO₂. Such decrease is the result of the CO₂ electro-reduction. A similar trend was reported by Koper.^[10] The CO₂ reduction has a higher thermodynamic potential barrier (-0.38 V vs. RHE) than HER, thus will decrease the total reduction rate if CO₂ is preferentially reduced at the expense of HER. To test the performance, the catalyst was kept at fixed potential and maintained for two hours in an H-shape two-compartment electrochemical cell. Figure 6b shows the chronoamperometry study of Pd/PANI at the fixed potential of -0.90 V in 0.5 M H₂SO₄ aqueous solution. It clearly shows a similar trend as the HER activity in Figure 5a that smaller Pd NPs gives higher current density.

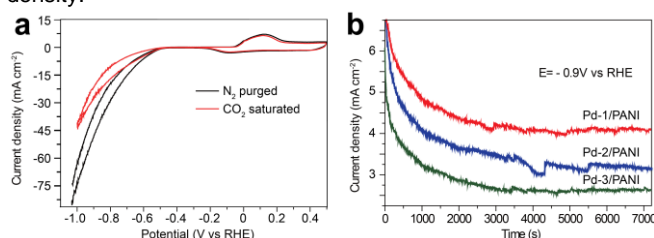


Figure 6. (a) CV plots of Pd-2/PANI in 0.5 M H₂SO₄ solution purged with N₂ and saturated with CO₂, the scan rate is 5 mV s⁻¹, the rotation speed is 500 rpm. (b) Chronoamperometry of Pd/PANI with potential fixed at -0.9 V in 0.5 M H₂SO₄ solution saturated with CO₂, rotation speed is 800 rpm.

The gas samples were also collected at different time periods for the analysis by gas chromatography (GC). The gaseous products mainly contained H₂ with a trace amount of CO. This reaffirmed that acidic conditions reduced the CO from CO₂, however, HER was still the dominant reaction.^[11]

The electrolyte after chronoamperometry study was analyzed using High-Performance Liquid Chromatography (HPLC) and ¹H-NMR. HCOOH and CH₃OH were clearly identified as the major products (in terms of carbon selectivity >95%) in the solution. Table 2 summarizes the catalytic performance data at -1.1 V vs. RHE.

Table 2. CO₂ electro-reduction results using PANI and Pd/PANI as electrocatalyst.

Catalyst	Applied potential (vs. RHE)	HCOOH production (μmol h ⁻¹)	CH ₃ OH production (μmol h ⁻¹)	Total charge (C)
PANI	-1.1	0.172	0	0.851
Pd-1/PANI	-1.1	4.01	0.203	11.45
Pd-2/PANI	-1.1	4.45	0.282	7.771
Pd-3/PANI	-1.1	2.42	0.187	5.492

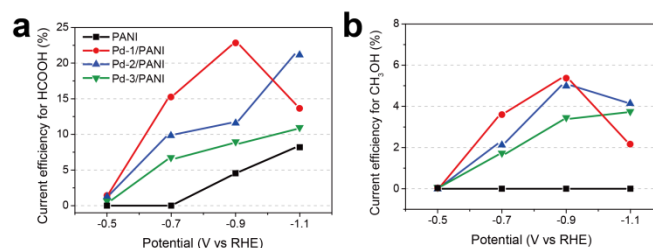


Figure 7. Current efficiency of CO₂ electro-reduction to (a) HCOOH and (b) CH₃OH. Same amount of PANI is used for all experiments. The electrolyte is 0.5 M H₂SO₄ solution and the reaction time is 120 min, the rotation speed is 800 rpm.

The current efficiencies (ϵ) of CO₂ electro-reduction to HCOOH and CH₃OH are shown Figure 7. From these test results, PANI can clearly act as an effective catalyst for the CO₂ reduction to HCOOH at -0.9 V and -1.1 V at the expense of HER but cannot produce CH₃OH at the given potential range. In contrast, Pd/PANI shows much higher activity towards HCOOH from -0.5 V to -1.1 V. When the potential is raised from -0.5 to -0.9, Pd/PANI material with smaller particle size shows higher current efficiency towards HCOOH production (highest ϵ at 22.8 % for Pd-1/PANI at -0.9 V). As far as we are aware, this high value of current efficiency, ϵ of 22.8% towards HCOOH at the expense of HER is unusual over Pd-1/PANI in acidic solution (cf. no HCOOH is produced over Pd/C) due to the suppression of HER by this material. However, when the potential is reached to -1.1 V, a dramatic decrease of ϵ for HCOOH production on Pd-1/PANI is taken place. At such a highly negative potential, the higher HER rate of Pd-1/PANI will take over (Figure 5). The efficiencies for CH₃OH formation on Pd/PANI catalysts with the different sizes are shown in Figure 7b. In general, the values are much lower compared to that for HCOOH production. Meanwhile, the data reflect the similar trend to that of Figure 7a. All Pd/PANI catalysts show increasing ϵ with increasing negative potential (from -0.5 V to -0.9 V). After reaching the highest ϵ value at 5.4%, it decreases to 2.0% at -1.1 V for Pd-1/PANI due to the take-off of the HER reaction. In compromise of the two catalysis reactions, Pd-2/PANI shows the highest ϵ value at -1.1 V. Clearly from the above studies, the use of smaller Pd NPs can exert stronger influence to PANI for higher conversions (current density values) and higher selectivities towards HCOOH and CH₃OH (current efficiency values) at the expense of HER. Thus, the results undoubtedly demonstrate that the size of Pd NPs can play a significant impact on activity and selectivity or current efficiency for catalytic CO₂ electro-reduction. The observation may be related to stronger catalytic/electronic effect exerted by smaller Pd NPs of higher surface energy and surface area or particularly exposed crystalline facet(s). Further study in this area is currently underway.

Conclusions

By controlling the synthesis parameters (temperature and adding rate), Pd/PANI samples with different Pd NPs sizes can

be prepared. Both PANI and Pd/PANI show similar nanofiber structure. Using UV-Vis, ATR-IR, and $^1\text{H-NMR}$ characterizations, it is concluded that Pd NPs can interact with PANI backbone via nitrogen atoms strongly, enabling electronic/catalytic interaction. It is clear from the results that the use of smaller Pd NPs exerts a stronger electronic interaction with PANI. These composite materials show a higher over-potential towards HER principally due to the reduction of ES to LEB in acidic media, indicative of HER as the competitive reaction in CO_2 electro-reduction can be suppressed in acidic condition. Catalytic CO_2 electro-reduction over these composites shows two main carbon-containing products in the electrolyte: HCOOH and CH_3OH and with a trace amount of CO in the gas phase. The size effect of Pd NPs in Pd/PANI is for the first time revealed on current density and current efficiency obtained: Pd/PANI with smaller Pd size shows higher current density and high current efficiency for both HCOOH and CH_3OH . However, if the negative potential is set beyond -0.9 V , HER can readily take off, resulting in lower efficiency for the two carbon containing products.

Experimental Section

Material synthesis

Chemicals: Ammonium persulfate (APS), HCl, $\text{NH}_3\cdot\text{H}_2\text{O}$, aniline, $(\text{NH}_4)_2\text{PdCl}_4$, Sodium borohydride (NaBH_4), Dimethylformamide (DMF) and 98% H_2SO_4 were used. All chemicals were purchased from Sigma-Aldrich and used as received. Distilled water (DI water) was used for washing. 18.5 M Ω Ultrapure water was utilized for all electrochemical measurements, and 0.5 M H_2SO_4 aqueous solution was used for electrochemical experiments.

PANI synthesis: The synthesis procedure of PANI nanofiber was adopted according to literature.^[20] Aniline (16 mmol) and Ammonium persulfate (APS) (4 mmol) were dispersed in 50 mL 1 M HCl aqueous solution, respectively. The two solutions were rapidly mixed with continuously stirring at 1000 rpm. The mixture was kept in an ice bath ($0\text{ }^\circ\text{C}$) for 24 h. The colour of the solution gradually changed from light yellow to dark green. After the reaction, the solution was filtered using a FluoroporeTM PTFE membrane filters (pore size 200 nm, from Sigma-Aldrich). Green residue was collected. Then, an excessive amount of 1 M $\text{NH}_3\cdot\text{H}_2\text{O}$ aqueous solution was used to wash the green residue until the colour turned to dark blue (de-doping process, from ES form to EB form). The residue was further washed using distilled water (DI water) 5 times until the filtrate turned colourless. The solid was collected and dried in an oven at $100\text{ }^\circ\text{C}$ overnight.

Pd/PANI synthesis: For the synthesis of Pd/PANI composite with different particle sizes, *in situ* reduction process was used. PANI powder (2 mmol of repeating unit, EB form) was dispersed in 25 mL DMF and sonicated for 30 min. Then, $(\text{NH}_4)_2\text{PdCl}_4$ (0.4 mmol) was added correspondingly to the suspension to prepare metal/PANI (molar ratio of metal/N = 1:5). The suspension was sonicated for another 30 min. NaBH_4 solution (1 g/mL in DMF) was introduced at specified temperature as reducing agent at specified dropping rate (Table 1), the molar ratio of NaBH_4 to metal ion was set at 15:1. The solution was stirred (500 rpm) and kept at room temperature for 5 h to ensure fully reduction of the metal precursor. The suspension was filtered, and the residue was washed 5 times with DI water. The solid was collected and dried in an oven at $100\text{ }^\circ\text{C}$ overnight.

Characterization methods

Electron microscopy: TEM, JEOL Model JEM-2100F; SEM, JEOL Model JSM-6335F.

X-ray diffraction (XRD): XRD analysis was carried out on a PANalytical X'Pert Pro diffractometer, the experiment is operated in the Bragg-Brentano focusing geometry and used $\text{Cu-K}\alpha$ radiation ($\lambda = 1.5418\text{ \AA}$) from a generator operating at 40 kV and 40 mA.

ATR-IR: The experiments were performed on a NICOLET 6700 instrument from Thermo Scientific. Specac's Golden GateTM Attenuated total reflectance (ATR) accessory (diamond crystal) was used with liquid nitrogen cooled MCT detector. IR spectra were collected for 64 scans with a resolution of 2 cm^{-1} .

$^1\text{H-Nuclear magnetic resonance}$ ($^1\text{H-NMR}$): 400 MHz instrument provided by Bruker.

High-Performance Liquid Chromatography (HPLC) and Gas chromatography: The experiments were done on an Agilent 1260 LC system. Flow rate was set at 0.25 mL min^{-1} . Mobile phase was 0.1 M H_2SO_4 solution. Agilent 7890B GC system was used for the gas detection.

Rotating disk electrode (RDE) preparation: For electrochemical testing of a catalyst, a glassy carbon rotating disk electrode (RDE) electrode was used with the diameter measured to be 7 mm (area 0.385 cm^2). The electrode was carefully polished using aqueous Al_2O_3 slurries (1 μm , 300 nm and 50 nm), and sonicated and washed using deionised water. The PANI and Pd/PANI samples were dispersed in DMF and sonicated for 1 h, with the concentration of 5 mg PANI mL^{-1} . Then 10 μL of the sample suspension was dropped on the electrode and the electrode was left to dry at room temperature for 60 mins.

Cyclic voltammetry (CV) and CO_2 electro-reduction: The electrochemical experiments were carried out using an RDE on a VersaSTAT 3 potentiostat provided by AMETEK, Princeton Applied Research. All experiments were done at room temperature using a Ag/AgCl (saturated KCl) reference electrode (0.198 V vs. RHE , room temperature) in 0.5 M H_2SO_4 solution. CV experiments were carried out in a one-compartment cell and CO_2 electro-reduction experiments were done in a H-shaped two-compartment cell, the total liquid volume of the cell was 10 mL. Platinum wire was used as counter electrode. The rotation speed of the RDE for CV experiments was set at 500 rpm, and the rotation speed of the RDE for CO_2 electro-reduction was 800 rpm. The scan rates were indicated in the figure captions. For CO_2 electro-reduction, CO_2 gas was bubbled through the solution for 1 h prior to the experiment to reach saturation. The electrode was then kept at a target potential (-0.5 V , -0.7 V , -0.9 V and -1.1 V vs. RHE) for 120 min, and CO_2 gas was continuously passed over the solution during this period. The final solution was collected and used for GC, HPLC, and NMR.

It should be noted that HER measurements were collected by the CV experiments in a single compartment cell. However, the testing experiments for CO_2 electro-reduction were done with the rotating disk electrode (GCE coated with Metal-PANI catalyst) in a two-compartment cell (not sealed) in order to reduce subsequent reactions on the counter electrode including methanol electro-oxidation and formic acid electro-oxidation. For the accurate determination of current density, it would be ideal to measure H_2 production together with the liquid products from CO_2 simultaneously in the same electrochemical cell. However, this could not be achieved since the present cell in rotating disk is not completely sealed.

There is also an anticipated difference in current density collected by CV plot and amperometric i-t plot which may not match in value to each other. The current density depends on capacitive current, electrochemical active surface and scan rate in CV. While electrochemical active surface plays the main role but scan rate cannot be the factor to influence on the overall current density in the case of amperometric i-t plot.

Keywords: polyaniline • palladium • size effect • CO₂ reduction • overpotential

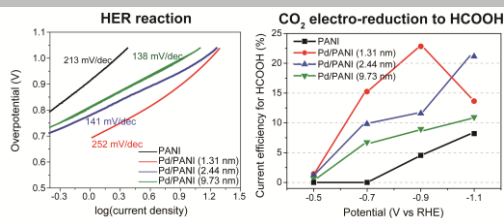
- [1] S. Enthaler, J. von Langermann, T. Schmidt, *Energy Environ. Sci.* **2010**, 3, 1207–11.
- [2] R. J. Lim, M. Xie, M. A. Sk, J. M. Lee, A. Fisher, X. Wang, K. H. Lim, *Catal. Today* **2014**, 233, 169–180.
- [3] J. Qiao, Y. Liu, F. Hong, J. Zhang, *Chem. Soc. Rev.* **2014**, 43, 631–675.
- [4] Q. Lu, J. Rosen, F. Jiao, *ChemCatChem* **2015**, 7, 38–47.
- [5] M. Azuma, K. Hashimoto, M. Hiramoto, M. Watanabe, T. Sakata, *J. Electrochem. Soc.* **1990**, 137, 1772–1778.
- [6] K. P. Kuhl, T. Hatsukade, E. R. Cave, D. N. Abram, J. Kibsgaard, T. F. Jaramillo, *J. Am. Chem. Soc.* **2014**, 136, 14107–14113.
- [7] X. Nie, M. R. Esopi, M. J. Janik, A. Asthagiri, *Angew. Chem., Int. Ed.* **2013**, 52, 2459–2462.
- [8] J. Albo, M. Alvarez-Guerra, P. Castaño, A. Irabien, *Green Chem.* **2015**, 17, 2304–2324.
- [9] B. I. Podlovchenko, E. A. Kolyadko, S. Lu, *J. Electroanal. Chem.* **1994**, 373, 185–187.
- [10] R. Kortlever, C. Balemans, Y. Kwon, M. T. M. Koper, *Catal. Today* **2015**, 244, 58–62.
- [11] D. Gao, J. Wang, H. Wu, X. Jiang, S. Miao, G. Wang, X. Bao, *Electrochem. Commun.* **2015**, 55, 1–5.
- [12] C. Henry, in *Nanomaterials and Nanochemistry*, Springer Berlin Heidelberg, Berlin, Heidelberg, **2008**, pp. 3–34.
- [13] W. Zhou, J. Y. Lee, *J. Phys. Chem. C* **2008**, 112, 3789–3793.
- [14] D. Gao, H. Zhou, J. Wang, S. Miao, F. Yang, G. Wang, J. Wang, X. Bao, *J. Am. Chem. Soc.* **2015**, 137, 4288–4291.
- [15] E. T. Kang, K. G. Neoh, K. L. Tan, *Prog. Polym. Sci.* **1998**, 23, 277–324.
- [16] K. Ogura, N. Endo, M. Nakayama, H. Ootsuka, *J. Electrochem. Soc.* **1995**, 142, 4026–4032.
- [17] F. Köleli, T. Röpke, C. H. Hamann, *Synth. Met.* **2004**, 140, 65–68.
- [18] C. Zhao, Z. Yin, J. Wang, *ChemElectroChem* **2015**, 2, 1974–1982.
- [19] A. G. Macdiarmid, J.-C. Chiang, M. Halpern, W.-S. Huang, S.-L. Mu, L. D. Nanaxakkara, S. W. Wu, S. I. Yaniger, *Mol. Cryst. Liq. Cryst.* **1985**, 121, 173–180.
- [20] J. Huang, R. B. Kaner, *J. Am. Chem. Soc.* **2004**, 126, 851–855.
- [21] J. P. Pouget, M. E. Jozefowicz, A. J. Epstein, X. Tang, A. G. Macdiarmid, *Macromolecules* **1991**, 24, 779–789.
- [22] W. S. Huang, A. G. Macdiarmid, *Polymer* **1993**, 34, 1833–1845.
- [23] J. E. Albuquerque, L. Mattoso, D. T. Balogh, R. M. Faria, J. G. Masters, A. G. Macdiarmid, *Synth. Met.* **2000**, 113, 19–22.
- [24] W. W. Focke, G. E. Wnek, Y. Wei, *J. Phys. Chem.* **1987**, 91, 5813–5818.
- [25] N. Pentland, J. O. Bockris, E. Sheldon, *J. Electrochem. Soc.* **1957**, 104, 182–194.
- [26] V. P. Indrakanti, J. D. Kubicki, H. H. Schobert, *Energy Environ. Sci.* **2009**, 2, 745–758.
- [27] E. M. Genies, M. Lapkowski, J. F. Penneau, *J. Electroanal. Chem. Interfacial Electrochem.* **1988**, 249, 97–107.

Entry for the Table of Contents (Please choose one layout)

Layout 1:

FULL PAPER

Pd/PANI shows unusual high over-potential of hydrogen evolution reaction (HER), which significantly suppresses the hydrogen formation in acidic media while encourages HCOOH and CH₃OH formation from CO₂. Decreasing Pd NPs size on PANI is shown to give increasing current efficiencies for HCOOH and CH₃OH from -0.5 V to -0.9 V but the use of higher potentials can cause severe HER activity.



Weiran Zhen, Ho Wing Man, Lin Ye*, Shik Chi Edman Tsang*

Page No. – Page No.

Title

Layout 2:

FULL PAPER

((Insert TOC Graphic here; max. width: 11.5 cm; max. height: 2.5 cm))

Author(s), Corresponding Author(s)*

Page No. – Page No.

Title

Text for Table of Contents